

Core-valence correlations for atoms with open shells

V. A. Dzuba and V. V. Flambaum

School of Physics, University of New South Wales, Sydney 2052, Australia

(Dated: February 2, 2008)

We present an efficient method of inclusion of the core-valence correlations into the configuration interaction (CI) calculations. These correlations take place in the core area where the potential of external electrons is approximately constant. A constant potential does not change the core electron wave functions and Green's functions. Therefore, all operators describing interaction of M valence electrons and $N - M$ core electrons (the core part of the Hartree-Fock Hamiltonian V^{N-M} , the correlation potential $\hat{\Sigma}_1(\mathbf{r}, \mathbf{r}', E)$ and the screening of interaction between valence electrons by the core electrons $\hat{\Sigma}_2$) may be calculated with all M valence electrons removed. This allows one to avoid subtraction diagrams which make accurate inclusion of the core-valence correlations for $M > 2$ prohibitively complicated. Then the CI Hamiltonian for M valence electrons is calculated using orbitals in complete V^N potential (the mean field produced by all electrons); $\hat{\Sigma}_1 + \hat{\Sigma}_2$ are added to the CI Hamiltonian to account for the core-valence correlations. We calculate $\hat{\Sigma}_1$ and $\hat{\Sigma}_2$ using many-body perturbation theory in which dominating classes of diagrams are included in all orders. We use neutral Xe I and all positive ions up to Xe VIII as a testing ground. We found that the core electron density for all these systems is practically the same. Therefore, we use the same $\hat{\Sigma}_1$ and $\hat{\Sigma}_2$ to build the CI Hamiltonian in all these systems ($M = 1, 2, 3, 4, 5, 6, 7, 8$). Good agreement with experiment for energy levels and Landé factors is demonstrated for all cases from Xe I to Xe VIII.

PACS numbers: PACS: 31.25.Eb, 31.25.Jf

I. INTRODUCTION

Accurate calculations for many-electron atoms play an important role in many advanced topics of modern physics. This includes parity and time invariance violating phenomena in atoms [1], search for manifestation of possible variation of fundamental constants in astrophysical data [2], or in present-day laboratory experiments [3], improving accuracy of atomic clocks [4], study of super-heavy elements (see, e.g. [5]), etc. Calculations are needed for planning of experiments and interpretation of the results.

Atoms of the most interest for the listed topics are usually found in the second part of the periodic table where measurements or observations are more likely to give useful information due to strong enhancement of the effects caused by interplay between relativistic and many-body effects. On the other hand, accurate treatment of relativistic and many-body effects represent a big challenge for atomic calculations. Not surprisingly, the number of methods capable of producing reliable and accurate results is very limited. The most advanced methods have been developed for atoms with one external electron above closed shells. For example, most accurate calculations of the parity non-conservation in cesium where carried out with two most advanced methods. One was the correlation potential (CP) method [6] combined with the all-order perturbation theory in screened Coulomb interaction [7] and the other was the linearized coupled cluster approach [8]. With these two methods, energy levels and transition amplitudes for alkali atoms can be calculated to the accuracy of fraction of percent while hyperfine structure and parity violating amplitudes are

calculated to the accuracy of 0.5 - 1% [7, 8, 9].

For atoms with more than one external electron in open shells the accuracy of calculations is significantly lower. For example, the best accuracy achieved for PNC in Tl is around 3% (3% in Ref. [10] and 2.5% in Ref. [11]). Typical accuracy for energies is about 1% or worse. The main challenge is the need for accurate treatment of both core-valence and valence-valence correlations. The most commonly used methods can be divided in several main groups: (a) many-body perturbation theory (MBPT) (see, e.g. [12]), (b) coupled cluster approach (CC) (see, e.g. [13]), (c) configuration interaction (CI) (see, e.g. [14]), and (d) multi-configuration Dirac-Fock method (MCDF)(see, e.g. [15]). There are also combinations of these basic techniques.

All of these method have their limitations. For example, CI usually treats correlations between valence electrons very accurately but core-valence correlations are either totally neglected or only small fraction of them is included. MBPT can include more core-valence correlations, but its application to the correlations between valence electrons is limited by the fact that these correlations are often too strong to be treated perturbatively. The CC approach includes certain types of core-valence and valence-valence correlations in all-orders and in principle can be formulated for any number of valence electrons. However, the equations are complicated and most of practical realization of the method deal with only one or two electrons (or an electron and a hole).

Significant progress can be achieved by combining different techniques. In 1996 we developed a method which combines the MBPT with the CI method (CI+MBPT) [16]. Here, the second-order MBPT was used to construct the effective Hamiltonian in the va-

lence space which includes the core-valence correlations. It differs from the standard CI Hamiltonian by an extra correlation operator $\hat{\Sigma}$ which accounts for the core-valence correlations. Single-electron part of this operator is very similar to the correlation potential used for atoms with one external electron [6]. It was demonstrated that inclusion of the core-valence correlations lead to a significant improvement of the accuracy of calculations (see, e.g. [16, 17, 18, 19]). Savukov and co-workers [20] developed a version of the method which uses the hole-particle formalism. They applied the technique for a calculation of the electron structure of the noble-gas atoms [20, 21].

The CI+MBPT method was successfully used for a number of atoms with two or three valence electrons [16, 17, 22] (or an electron and a hole [20, 21]). Its extension to atoms with more electrons in open shells meets some difficulties. It turns out that convergence of the MBPT varies very much from atom to atom and strongly depends on an initial approximation. The core-valence correlations are often too large if treated in the same fashion as in our original works and their inclusion does not improve the results.

It is widely accepted that the Hartree-Fock potential is the best choice as a zero approximation for consequent use of the MBPT due to great reduction of the terms caused by exact cancellation between the potential and electron-electron Coulomb terms. However, for atoms with open shells HF procedure is not defined unambiguously. This is especially true when the CI method is to be used. Here we have freedom of how many electrons are to be included into the initial HF procedure and how many electrons are to be treated as valence electrons in the CI calculations. It was found in our previous work [23] that for a wide range of atoms the best choice is the so-called V^{N-M} approximation. These are the atoms in which valence electrons form a separate shell, defined by the same principal quantum number. For example, the ground state configuration of xenon is [Pd] $5s^25p^6$. Its eight outermost electrons have $n = 5$ while all other electrons have $n < 5$. This means that eight outermost electrons should be treated as valence electrons and the initial HF procedure should not include them. This greatly simplifies the MBPT, improves its convergence and allows one to include higher-order correlations in the same way as it was done for atoms with one external electron.

The aim of the present work is to develop a solid theoretical background for use of the V^{N-M} potential as a starting point. In principle, this starting point is equivalent to any other choice of the initial HF potential. Indeed, the actual role of the *subtraction diagrams* in the correlation operators $\hat{\Sigma}$ is to reduce results obtained with any zero approximation to V^{N-M} results (see an explanation below). However, the technique for V^{N-M} is much simpler (no subtraction diagrams) and allows us to sum dominating chains of higher order diagrams to all orders (it is practically impossible for other choice of zero approximation). This results in a higher accuracy. Another advance of the present work is the use

of a compact basis for valence states. In our previous works [22, 23, 24, 25] we used the same basis to calculate $\hat{\Sigma}$ and to do the CI calculations. The basis was formed from the eigenstates of the \hat{V}^{N-M} potential. This had an advantage of having the same single- and double-electron matrix elements for all ions of the same atom. Moving from ion to ion was easy, requiring only change the number of electrons in the CI calculations. However, convergence of the CI calculations rapidly deteriorated with growing number of electrons. When number of electrons became as large as eight, saturation of the basis was very hard to achieve unless huge computer resources were used. In present work we demonstrate that the basis states for valence electrons don't have to be eigenstates of the \hat{V}^{N-M} potential. Instead, HF states calculated in the mean field of all electrons (of a neutral atom or corresponding positive ion) can be used after minor modifications. In this case we have to recalculate the CI basis when we change the number of valence electrons M . However, the gain is much larger. Since HF states are already good approximations to the wave functions of valence electrons we can limit the basis to just few states in each partial wave. Therefore, even for eight valence electrons the CI matrix is small, its calculation and diagonalization takes little time but the final results are very accurate.

We calculate energy levels and Landé g -factors for neutral xenon and all its positive ions from X II to Xe VIII for illustration on how the technique works. Good agreement with experiment is demonstrated for all cases while very little computer resources are needed on every stage of the calculations.

II. CORE ELECTRON DENSITY AND POTENTIAL IN V^{N-M} AND V^N APPROXIMATIONS

The effective Hamiltonian of the CI method has the form (see, e.g. [16])

$$\hat{H}^{\text{eff}} = \sum_{i=1} \hat{h}_{1i} + \sum_{i < j} \frac{e^2}{|\mathbf{r}_i - \mathbf{r}_j|}. \quad (1)$$

Summation goes over valence electrons, $\hat{h}_1(r_i)$ is the one-electron part of the Hamiltonian

$$\hat{h}_1 = c\alpha\mathbf{p} + (\beta - 1)mc^2 - \frac{Ze^2}{r} + V_{\text{core}}, \quad (2)$$

α and β are the Dirac matrices, Ze is the nuclear charge and V_{core} is the electrostatic potential created by the core electrons. Regardless of initial approximation used to calculate core and valence states, the valence electrons never contribute to V_{core} directly. They can only contribute to V_{core} via the self-consistent HF procedure or via any other potential used to represent valence electrons. If the core electrons and valence electrons belong to different shells the effect of the valence electrons on

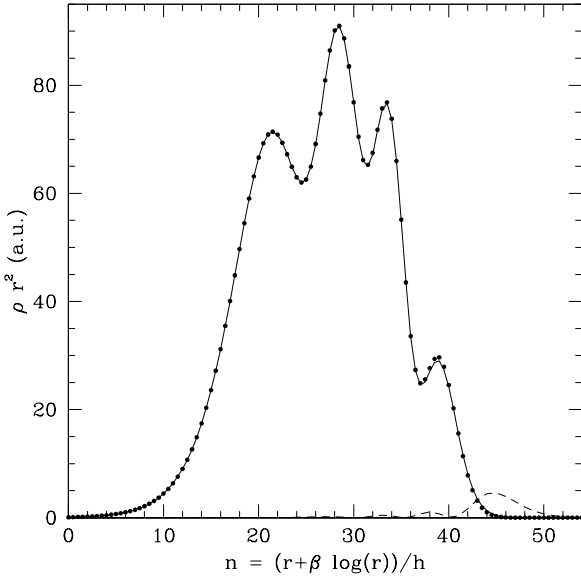


FIG. 1: Electron densities (multiplied by r^2) of Xe I and Xe IX. Atomic core ($n=1,2,3,4$) of Xe I, solid line; 5s and 5p, dashed line; electron density of Xe IX, dots.

electron states in the core and thus on V_{core} can be extremely small. Indeed, in this case the overlap between density of the valence electrons and density of the core electrons is small. Therefore, the exchange interaction between the core and valence electrons, which is proportional to the overlap, is negligible in comparison with energy of the core electrons. On the other hand, the direct potential created by the valence electrons is practically constant inside the core since nearly all charge of the valence electrons is located outside the core. Constant potential corresponds to zero electric field and cannot have any effect on the wave function of the core electrons. The only effect of the constant potential V_0 is in energy shift $\delta E = V_0$. However, it does not change the single-particle wave functions and Green's functions of core electrons since the wave equation contains the difference $E - V_0$ which does not change. We may formulate this conclusion using the perturbation theory. In first order in V_0 a core state a in the V^{N-M} approximation and \tilde{a} in the V^N approximation are related by

$$|\tilde{a}\rangle = |a\rangle + \sum_n \frac{\langle a|V_0|n\rangle}{E_a - E_n} |n\rangle. \quad (3)$$

If the potential V_0 is constant, the matrix element $\langle a|V_0|n\rangle = V_0\langle a|n\rangle = 0$ due to the orthogonality condition. This explains why the changes of the core wave functions, density and potential are very small.

Small overlap between the core and valence states usually takes place when these states correspond to different atomic shells defined by the principal quantum number (see, e.g. [23, 24, 25]). In case of xenon, eight outermost electrons have principal quantum number $n = 5$ (the

$5s^25p^6$ ground state configuration), while all core electrons have $n < 5$. Therefore, if the eight electrons are considered to be valence electrons we should expect that they have little effect on the core states. Fig. 1 shows electron densities of Xe I and Xe IX calculated in the HF approximation. For the neutral Xe I electron densities of valence and core electrons are shown separately. One can see that the overlap between them is indeed very small. Therefore, it turns out that when electron density of Xe IX is calculated it practically coincides with the electron density of the core states of neutral Xe. The former is shown by dots of Fig. 1. Resolution of this figure doesn't allow us to see any difference between electron densities of Xe IX and the core of Xe I. This is in spite of huge difference in energies of core states of two atoms. One may argue that huge difference in energies should lead to a noticeable difference in wave functions, at least on large distances. Indeed, a wave function of an atomic electron has asymptotic defined by its energy and potential

$$\psi(r) \sim e^{-\int \sqrt{2m(E-V(r))} dr}. \quad (4)$$

However, in the area up to the radius of the valence shell there is actually no difference in $E - V(r)$ for the core orbitals in Xe IX and Xe I since $\delta E = \langle \delta V \rangle$. The difference in asymptotic behavior appears only near the radius of the valence shell where the core electron density is extremely small.

Thus we conclude that the core electron density and potential have practically no dependence on the number of valence electrons if the valence electrons are in a different shell.

III. THE CORE-VALENCE CORRELATION CORRECTIONS IN THE V^N AND V^{N-M} APPROXIMATIONS

The use of the Feynman diagram technique allows us to express the core-valence correlation corrections in terms of the single-particle wave functions and Green's functions [7] (see Appendix). Therefore, all the arguments presented above are applicable when we consider calculation of the correlation operators $\hat{\Sigma}_1$ and $\hat{\Sigma}_2$; they may be calculated using V^{N-M} basis for core electrons.

It may be instructive to clarify this conclusion using more popular Schroedinger perturbation theory where explicit summation over intermediate states is involved. The correlations between the valence and core electrons as well as the screening of the interaction between the valence electrons happen inside the area occupied by the core electrons. Let us enclose the core by a sphere with zero boundary condition for the core electrons. This allows us to reduce the core electron problem to the discrete spectrum. Let us now consider the interaction of the core electrons with external electrons using the perturbation theory. The constant potential V_0 of external electrons does not change the core electron wave functions. It also

does not change the energy differences $E_n - E_m$ between the enclosed “core” states, they are shifted by the same energy V_0 (note that these enclosed states form complete basis set inside the sphere). Therefore, all the terms in the perturbation theory for the core-valence interaction (beyond the mean field which we take into account in the V^N valence orbitals) do not depend on the spectator valence electrons. This is why we can calculate all core-valence correlations using the V^{N-M} core orbitals. To avoid misunderstanding we should note that we use this picture for the explanation only, no special boundary conditions for core electrons are needed for actual calculations (it is obvious if we use the Green’s function technique; all the integrals over coordinates are dominated by the core area where the correlations between the valence and core electrons actually happen). Note that below we do not neglect effects of V_0 , we only treat them as a perturbation since the non-diagonal matrix elements $\langle a|V_0|n \rangle$ are small.

The effective Hamiltonian of the CI+MBPT method has the form similar to (1) but with extra terms for single and double electron parts of it. These terms, for which we use notation $\hat{\Sigma}$, describe the core-valence correlations [16]. There is a single-electron operator $\hat{\Sigma}_1$ which is added to the single-electron part \hat{h}_1 (2) of the CI Hamiltonian:

$$\hat{h}_1(r) \rightarrow \hat{h}_1 + \hat{\Sigma}_1. \quad (5)$$

$\hat{\Sigma}_1$ describes correlations between a particular valence electron and core electrons. It is very similar to the correlation potential $\hat{\Sigma}$ used for atoms with one external electron (see, e.g. [6]).

There is also a two-electron operator $\hat{\Sigma}_2$ which modifies Coulomb interaction between valence electrons:

$$\frac{e^2}{|\mathbf{r}_1 - \mathbf{r}_2|} \rightarrow \frac{e^2}{|\mathbf{r}_1 - \mathbf{r}_2|} + \hat{\Sigma}_2. \quad (6)$$

Physical interpretation of $\hat{\Sigma}_2$ is the screening of Coulomb interaction between valence electrons by core electrons.

When number of valence electrons is greater than 2 there is also a three-body operator $\hat{\Sigma}_3$ [16] and higher-order many-body operators $\hat{\Sigma}_4$, $\hat{\Sigma}_5$, etc. . However, they are usually very small and we will not consider them in the present work.

The full set of diagrams for $\hat{\Sigma}_1$ and $\hat{\Sigma}_2$ in the second order of MBPT is presented on Figs. 2, 3, 4 and 5. It contains the so-called *subtraction* diagrams which are proportional to $V_{\text{core}} - V^{\text{HF}}$, where V_{core} is the potential of the core electrons as in the effective CI Hamiltonian (1), V^{HF} is the potential in which states of the core were calculated. Note that subtraction diagrams vanish in the V^{N-M} approximation: $V_{\text{core}} = V^{\text{HF}}$.

The origin of the subtraction diagrams is clear from the definition of the perturbation (residual interaction) operator $U = H_{\text{exact}} - H_0$ where H_{exact} is the exact Hamiltonian and H_0 is the zero approximation Hamiltonian. If the field of external electrons is included in H_0 it

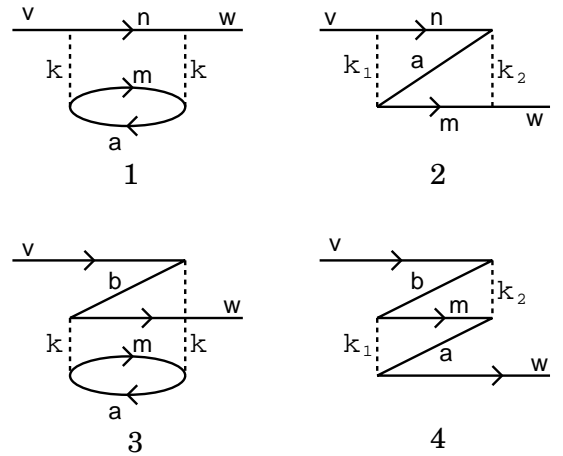


FIG. 2: Second-order diagrams for single-electron correlation operator $\hat{\Sigma}_1^{(2)}$.

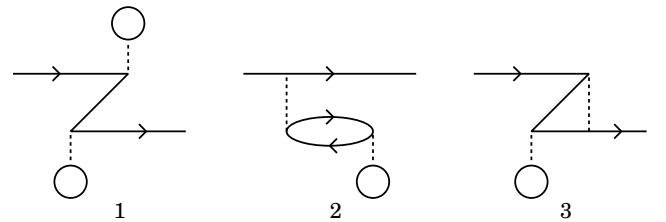


FIG. 3: Subtraction diagrams for $\hat{\Sigma}_1^{(2)}$.

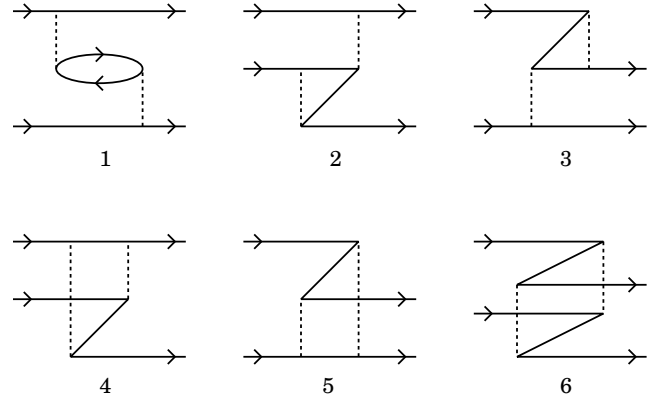


FIG. 4: Second-order diagrams for double-electron correlation operator $\hat{\Sigma}_2^{(2)}$.

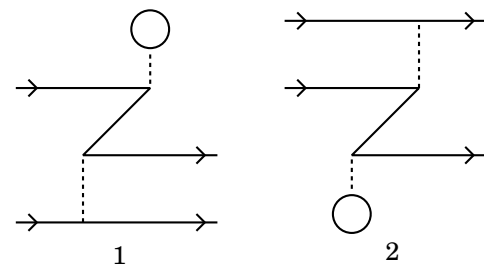


FIG. 5: Subtraction diagrams for $\hat{\Sigma}_2^{(2)}$.

produces additional contributions which we call the subtraction diagrams. Thus, the potential V_0 appears with positive sign in the mean field (and core wave functions), and with negative sign in the residual interaction (and subtraction diagrams). If we calculate all correlations exactly, to all orders, V_0 must disappear in the final result. In any finite order of the many-body perturbation theory there are only partial cancellations; lower orders of expansion in V_0 are canceled out. Thus, the role of the subtraction diagrams is to cancel the potential of spectator valence electrons acting on the core electrons (effect of valence electrons on the core lines of the diagrams). In other words, the subtraction diagrams guarantee that in any given order of expansion in V_0 the operators $\hat{\Sigma}_1$ and $\hat{\Sigma}_2$ are reduced to the results of V^{N-M} approximation. Therefore, if the non-diagonal matrix elements of V_0 are small the V^{N-M} approximation is the best zero approximation since the calculations are much simpler (no subtraction diagrams).

It is easy to see all these cancellations of V_0 explicitly, order by order in V_0 . Here one should remember that change of the valence electron energies due to change of the core Hartree-Fock potential (which formally has the first order in the Coulomb interaction) is actually canceled by the second order subtraction diagrams; contribution of V_0 into the core wave functions in the second order diagrams is canceled by the third order subtraction diagrams, etc.

IV. HIGHER ORDER TERMS IN $\hat{\Sigma}$

We have seen above that if the electrostatic potential V_0 created by valence electrons is nearly constant inside the core then the V^{N-M} approximation is equivalent to the $V^{N-M} + V_0$ approximation, where V_0 can have contributions from all M valence electrons, or any fraction on them or it can be just a model potential. The only condition is that V_0 is nearly constant inside the core. This means that without any compromise on accuracy we can do the calculation in the V^{N-M} approximation which is technically more simple. Another advantage of using V^{N-M} is that we have the same effective Hamiltonian for any number of valence electrons from 1 to M . Therefore we can do the calculations in a very similar way for all corresponding ions as well as for a neutral atom.

Eliminating subtracting diagrams in the V^{N-M} approximation makes $\hat{\Sigma}_1$ practically identical to the correlation potential $\hat{\Sigma}$ used for atoms with one external electron. Therefore, we can try to improve the accuracy of calculations by including important higher order terms into $\hat{\Sigma}_1$ the same way as it was done in a number of calculations for alkali atoms (see, e.g. [7, 9]). We include two dominating classes of higher order diagrams into calculation of $\hat{\Sigma}_1$. One is screening of the Coulomb interaction between valence and core electrons by other core electrons. Another is interaction between an elec-

TABLE I: Removal energies of lowest states of Xe VIII (cm^{-1}) in different approximations; comparison with experiment

State	HF	$\hat{\Sigma}^{(2)}$	$\hat{\Sigma}^{(\infty)}$	Expt [26]
$5s_{1/2}$	839764	858722	854842	854755
$5p_{1/2}$	725342	741343	738280	738288
$5p_{3/2}$	707377	722378	719550	719703
$5d_{3/2}$	536494	546174	544092	544867
$5d_{5/2}$	533632	543150	541096	541939
$4f_{5/2}$	572050	590725	587324	589594
$4f_{7/2}$	571684	590056	586717	589044

tron excited from the core and a hole in the core created by this excitation. Both classes of diagrams are included in all orders (see, e.g. [7, 9] for details).

We use notation $\hat{\Sigma}_1^{(\infty)}$ for the all-order $\hat{\Sigma}$ operator as compared to $\hat{\Sigma}_1^{(2)}$ for the second-order operator. The effect of inclusion of second and higher order correlations can be illustrated by calculating of the energy levels of Xe VIII. This ion has only one valence electron and calculations for it can be done the same way as for other single-valence electron atoms (see, e.g. [7]). Instead of diagonalizing the CI matrix we solve HF-like equations for valence electrons in coordinate space, with $\hat{\Sigma}_1$ included in it:

$$(h_1 + \hat{\Sigma}_1 - \epsilon)\psi = 0. \quad (7)$$

Here single-electron Hamiltonian h_1 is given by (2) while $\hat{\Sigma}_1$ can be either $\hat{\Sigma}_1^{(2)}$ or $\hat{\Sigma}_1^{(\infty)}$. If no $\hat{\Sigma}_1$ is included then eq. (7) gives HF energies and wave functions.

The results of calculations are presented in Table I and compared with experiment. One can see systematic significant improvement of the results when first $\hat{\Sigma}_1^{(2)}$ and then $\hat{\Sigma}_1^{(\infty)}$ are included.

We are now going to use the same $\hat{\Sigma}_1^{(\infty)}$ operator for all ions from Xe VII to Xe II and for neutral xenon. For all these ions which have more than one valence electrons the $\hat{\Sigma}_2$ operator should also be included. In the V^{N-M} approximation the $\hat{\Sigma}_2$ term is given by diagrams on Fig. 4, and no subtraction diagrams are needed. To include higher-order correlations into $\hat{\Sigma}_2$ we use screening factors the same way as we do this for the exchange diagrams of $\hat{\Sigma}_1$ (Figs. 2.2 and 2.4) (see, e.g. [7]). To explain how screening factors are found and used we need to go into more details on how the all-order correlation operator $\hat{\Sigma}_1^{(\infty)}$ is calculated. We use Feynman diagram technique to calculate *direct* diagrams (Fig. 2.1 and 3). It allows us to include an infinite chain of screening diagrams in all orders [7]. Application of the Feynman diagram technique to *exchange* diagrams (Fig. 2.2 and 4) is much more complicated [9]. On the other hand these diagrams are usually an order of magnitude smaller than *direct* diagrams. Therefore it makes sense to use an approximate method by introducing *screening factors*. We assume that screening of Coulomb interaction between

TABLE II: Basis states of valence electrons used in the CI calculations, their total number (N) for each atom or ion and HF configurations in which they were calculated

Atom	N	Basis states	Configurations
Xe I	15	5s,6s,7s,5p,6p,7p,5d,6d,4f	$5s^25p^6,$ $5s^25p^5n$
Xe II	10	5s,6s,5p,6p,5d,4f	$5s^25p^5,$ $5s^25p^4n$
Xe III	8	5s,6s,5p,6p,5d	$5s^25p^4,$ $5s^25p^3n$
Xe IV	10	5s,6s,5p,6p,5d,4f	$5s^25p^3,$ $5s^25p^2n$
Xe V	8	5s,6s,5p,6p,5d	$5s^25p^2,$ $5s^25pn$
Xe VI	8	5s,6s,5p,6p,5d	$5s^25p,$ $5s^2n$
Xe VII	8	5s,6s,5p,5d	$5s^2,$ $5snl$

core and valence electrons depends only on multipolarity k of Coulomb interaction. Screening factors f_k are calculated as ratios of partial contributions to $\hat{\Sigma}_1$:

$$f_k = \langle \hat{\Sigma}_k^{(\infty)} \rangle / \langle \hat{\Sigma}_k^{(2)} \rangle, \quad (8)$$

where only *direct* diagrams are included in $\hat{\Sigma}_k^{(2)}$ and $\hat{\Sigma}_k^{(\infty)}$ and only screening of Coulomb interaction but no hole particle interaction is included in $\hat{\Sigma}_k^{(\infty)}$. The values of f_k found from calculations for alkali atoms are

$$\begin{aligned} f_0 &= 0.72, & f_1 &= 0.62, & f_2 &= 0.83, \\ f_3 &= 0.89, & f_4 &= 0.94, & f_5 &= 1.00, \text{ etc.} \end{aligned} \quad (9)$$

The values of f_k change very little from atom to atom and the values presented above can be used for xenon. This is supported by the results obtained for Xe VIII (see Table I).

The effect of $\hat{\Sigma}_2$ on atomic energies is much smaller than those of $\hat{\Sigma}_1$. Therefore we can also treat higher-order correlations in $\hat{\Sigma}_2$ in an approximate way, via screening factors, as we do this for exchange part of $\hat{\Sigma}_1$. We replace every Coulomb integral Q_k on all diagrams on Fig. 4 except diagram Fig. 4.1 by its screened values $f_k Q_k$ where screened factors f_k are taken as in (9). For the diagram Fig. 4.1 only one of the Coulomb integrals is replaced by its screened value. This is because this diagram can generate only one infinite chain of loops representing screening. Therefore, screening should be included only once. This is very similar to the all-order treatment of the direct diagram for $\hat{\Sigma}_1$ (Fig. 2.1 and 2.3). If this diagram is expressed in terms of screened Coulomb interaction, only one of two Coulomb integrals should be replaced by a screened one (see [7, 9] for details).

V. BASIS

There are two single-electron basis sets in this problem. One is used to calculate $\hat{\Sigma}$ and other is used to construct many-electron states of valence electrons for the CI calculations.

In principle, it is possible to use the same basis for both purposes and we did so in many of our earlier calculations [17, 22, 23, 24, 25]. The most convenient choice for

the basis is the basis consisting of single-electron states calculated in the V^{N-M} potential. We use B-spline technique to calculate the basis. Lower and upper component of each basis set is expressed as linear combination of 40 B-splines in the cavity of radius of $40a_B$. Expansion coefficients are found from the condition that the basis states are the eigenstates of HF Hamiltonian (2) with the V^{N-M} potential. The advantages of this approach are many: core and valence states are orthogonal automatically, the basis is reasonably complete and does not depend on number of valence electrons. The latter means in particular that if we want to change number of valence electrons (e.g. to do calculation for another ion) we don't have to recalculate single and double electron matrix elements. The shortcoming of this approach is rapid increase of the size of the CI matrix with the number of valence electrons. Indeed, typical number of single-electrons basis states needed to get saturation of the basis is around 100. The number of ways, valence electrons can be distributed over these 100 states grows very fast with the number of valence electrons. For eight electrons like for Xe I the matrix reaches unmanageable size, even when some configuration selection technique is used.

In present work we use the basis described above only for calculation of $\hat{\Sigma}$. For the CI calculations we use very compact basis of HF states of corresponding ion or neutral atom. For example, we perform HF calculations for neutral Xe I in its ground state $[Pb]5s^25p^6$ in the V^N approximation and then use the $5s$ and $5p$ states as the basis states for the CI calculations for Xe I in the V^{N-8} approximation. Other basis states like $6s$, $6p$, etc. are obtained by removing one $5p$ electron from the atom and calculating these states in the frozen field of remaining electrons. The states obtained this way are not orthogonal to the core which corresponds to the V^{N-8} potential. In the relativistic case the basis states for valence electrons must also be orthogonal to the negative energy states (positron states). Both conditions (orthogonality to the core and to the negative energy states) can be achieved by projecting a basis state on the B-spline states above the core:

$$|v\rangle \rightarrow |v'\rangle = \sum_i |i\rangle \langle i|v\rangle. \quad (10)$$

Here summation goes over states above the core. Functions $|v'\rangle$ are more suitable for the CI calculations than states $|v\rangle$ because they don't have admixture of the core and negative energy states.

If more than one state of particular symmetry is included into the basis (like, e.g. the $6p$ and $7p$ states for Xe I) they also need to be orthogonalized to each other.

Full list of valence states for xenon and its ions used in the calculations are presented in Table II. First column shows an atom or ion, second column gives total number of valence basis states, then states are listed together with the configurations in which they were calculated.

Note that every state with $l > 0$ consists of two function, e.g. $6p$ stands for $6p_{1/2}$ and $6p_{3/2}$, etc. Note also that the number of basis states is always small, much smaller than about 100 needed with the B-spline basis. This greatly overweights an inconvenience of recalculating the basis for every ion or atom.

VI. CALCULATIONS FOR XENON AND ITS IONS

In this section we present calculations for xenon and its ions. The whole calculation scheme consists of the following steps (we use Xe I as an example):

1. HF for Xe IX, V^{N-8} potential is obtained.
2. Calculation of B-spline states in the V^{N-8} potential.
3. Calculation of $\hat{\Sigma}_1$.
4. HF for Xe I, the $5s$ and $5p$ basis states are obtained.
5. Calculation of valence basis states.
6. Calculation of single and double-electron matrix elements, including matrix elements of $\hat{\Sigma}_2$.
7. Calculation and diagonalization of the CI matrix.

At first glance this scheme doesn't look very simple. However, none of the steps listed above are very time consuming or require large computer power. The most time consuming step is calculation of $\hat{\Sigma}$ ($\hat{\Sigma}_1$ in step 3 and $\hat{\Sigma}_2$ in step 6). An efficient way of calculating both $\hat{\Sigma}_1$ and $\hat{\Sigma}_2$ is presented in the appendix. The timescale to obtain all results presented in this section while using a PC or a laptop is one day.

Results for neutral xenon are presented in Table III while results for six positive ions from Xe VII to Xe II are presented in Tables IV, V, VI, VII, VIII and IX. For neutral xenon (Table III) we study in detail the role of core-valence correlations by including them in different approximations. The basis for valence states is kept the same in all cases (see previous section for the description of the basis). The approximations are

1. First, we present the results of the standard CI method, with no core-valence correlations (the "CI" column of Table III). Accuracy for the energies as compared to experimental values are not very good. However the difference does not exceed 10% which is sufficiently good for many applications. This is in spite of the fact that calculations for neutral xenon were done with atomic core corresponding to highly ionized Xe IX. This is another confirmation that change in the core potential V_{core} from Xe I to Xe IX is very small.

2. Second-order $\hat{\Sigma}_1^{(2)}$ is added to the effective Hamiltonian (the " $\hat{\Sigma}_1^{(2)}$ " column of Table III). The results are significantly closer to the experiment but the correction is too large. This is similar to what usually takes place with the second-order correlation correction for atoms with one external electron.
3. Second-order $\hat{\Sigma}_2^{(2)}$ is also added (the " $\hat{\Sigma}_1^{(2)} \& \hat{\Sigma}_2^{(2)}$ " column). As one can see $\hat{\Sigma}_2^{(2)}$ acts in opposite direction to $\hat{\Sigma}_1^{(2)}$ and the results are even closer to the experiment.
4. Higher orders are included in $\hat{\Sigma}_1$ while $\hat{\Sigma}_2$ is not included at all (the " $\hat{\Sigma}_1^{(\infty)}$ " column). The effect of higher orders in $\hat{\Sigma}_1$ is numerically close to the effect of $\hat{\Sigma}_2$ as is evident from the comparison with previous column. This coincidence is accidental.
5. Higher orders are included in $\hat{\Sigma}_1$ while $\hat{\Sigma}_2$ is included in second order (the " $\hat{\Sigma}_1^{(\infty)} \& \hat{\Sigma}_2^{(2)}$ " column). The results are improved but for many states the correction is too large.
6. Higher orders are included in both $\hat{\Sigma}_1$ and $\hat{\Sigma}_2$ (the " $\hat{\Sigma}^{(\infty)}$ " column). This is the most complete calculation we have in present work. Here we also included calculated values of Landé's g -factors. The g -factors are very useful for identification of the states, especially for atoms with dense spectrum where calculations do not always reproduce the correct order of the levels.

The last column of Table III presents the difference between experimental and calculated energies where calculated energies correspond to the most complete calculation ($\hat{\Sigma}^{(\infty)}$): $\Delta = E_{expt} - E_{calc}$. This difference does not exceed 2% and should mostly be attributed to incompleteness of the basis. Indeed, it is hard to expect that the basis consisting of only 15 single-electron states (from one to three in each partial wave from $l = 0$ to $l = 3$) to be complete. Test calculations show that adding more states to the basis do have some effect on the energies of the states. The effect is larger for higher states. For example, it is hard to expect any reasonable accuracy for the states of the $5s^2 5p^5 6d$ configuration without having the $6d$ state in the basis. But adding the $6d$ state to the basis also have some effect on the lower $5s^2 5p^5 5d$ configuration. The detailed study of the ways to saturate the basis goes beyond the scope of the present work.

Tables IV, V, VI, VII, VIII and IX. present our results for xenon positive ions from Xe VII to Xe II. Only results obtained in the "best" approximation ($\hat{\Sigma}^{(\infty)}$) are included. Calculations for the ions start from point 4 in the scheme presented in the beginning of this section. This is because first 3 points are exactly the same as for neutral xenon. Note that one of the most time consuming steps, calculation of $\hat{\Sigma}_1$, doesn't need to be repeated. Basis states for valence electrons used in the CI calculations are described in previous section (see Table II). We

TABLE III: Ground state removal energy (a.u.), excitation energies (cm^{-1}) and g -factors of lowest states of Xe in different approximations

State		J	CI	$\hat{\Sigma}_1^{(2)}$	$\hat{\Sigma}_1^{(2)} \& \hat{\Sigma}_2^{(2)}$	$\hat{\Sigma}_1^{(\infty)}$	$\hat{\Sigma}_1^{(\infty)} \& \hat{\Sigma}_2^{(2)}$	$\hat{\Sigma}^{(\infty)}$		Expt		
				E	E	E	E	E	g	E	g	Δ
$5s^2 5p^6$	1S	0	-15.21	-15.76	-15.69	-15.53	-15.48	-15.49		-15.61		
$5s^2 5p^5 6s$	$^2[3/2]^o$	2	62710	70595	68587	68289	66310	67040	1.4994	67068	1.50095	28
		1	64013	71916	69873	69594	67573	68319	1.2157	68045	1.2055	-274
$5s^2 5p^5 6s$	$^2[1/2]^o$	0	71616	80192	78425	77568	75824	76480	0	76197		-283
		1	72896	81586	79764	78925	77120	77799	1.3160	77185	1.321	-614
$5s^2 5p^5 6p$	$^2[1/2]$	1	72707	81332	79318	78519	76533	77283	1.8559	77269	1.852	-14
		0	76219	84202	82183	81602	79607	80350	0.0000	80119		-231
$5s^2 5p^5 6p$	$^2[5/2]$	2	73810	82369	80304	79587	77545	78307	1.1005	78120	1.11103	-187
		3	74045	82627	80568	79837	77802	78564	1.3333	78403	1.336	-161
$5s^2 5p^5 6p$	$^2[3/2]$	1	74755	83339	81261	80549	78496	79260	1.0232	78956	1.02348	-304
		2	74964	83540	81466	80755	78705	79468	1.3913	79212	1.3836	-256
$5s^2 5p^5 5d$	$^2[1/2]^o$	0	76068	84821	82949	82082	80235	80919	0	79771		-1148
		1	76259	84946	83067	82221	80367	81054	1.3786	79987	1.395	-1067
$5s^2 5p^5 5d$	$^2[7/2]^o$	4	76425	84622	82869	81997	80257	80900	1.2500	80197	1.2506	-703
		3	77283	85513	83764	82877	81141	81783	1.0762	80970	1.0749	-813
$5s^2 5p^5 5d$	$^2[3/2]^o$	2	76370	84667	82973	82001	80323	80947	1.3775	80323	1.3750	-624
		1	80595	89175	86989	86445	84279	85087	0.9900	83890		-1197
$5s^2 5p^5 5d$	$^2[5/2]^o$	2	78310	86627	84853	83959	82199	82846	0.9419	81926		-920
		3	78626	86996	85209	84306	82531	83184	1.2179	82430		-754
$5s^2 5p^5 7s$	$^2[3/2]^o$	2	80504	89101	86967	86367	84254	85042	1.4910	85189		147
		1	81064	89742	87648	86951	84880	85655	0.9759	85440		-215
$5s^2 5p^5 7p$	$^2[1/2]$	1	83048	91935	89859	89051	87001	87773	1.7930	87927	1.7272	154
		0	84221	92910	90834	90110	88057	88825	0	88842		17
$5s^2 5p^5 7p$	$^2[5/2]$	2	83464	92252	90160	89397	87330	88104	1.1107	88352	1.1276	248
		3	83558	92350	90262	89494	87429	88204	1.3333	88469	1.330	265
$5s^2 5p^5 6p$	$^2[3/2]$	1	83700	92521	90429	89662	87594	88369	1.0216	88379	0.7925	10
		2	84883	94445	92365	91398	89352	90122	1.1497	89162	1.190	-960
$5s^2 5p^5 6d$	$^2[1/2]^o$	0	83637	92398	90367	89562	87557	88309	0	88491		182
		1	83728	92489	90466	89654	87658	88405	1.3430	88550		145
$5s^2 5p^5 7p$	$^2[3/2]$	2	83832	92610	90519	89759	87693	88466	1.3843	88687	1.3520	221
		1	84392	94128	92055	90956	88909	89680	0.6345	88745	0.9039	-935
$5s^2 5p^5 6d$	$^2[3/2]^o$	2	83947	92702	90695	89870	87892	88632	1.3165	88708		76
		1	86666	95327	93442	92542	90699	91378	0.6980	90032		-1346
$5s^2 5p^5 6d$	$^2[7/2]^o$	4	84071	92767	90743	89952	87956	88701	1.2500	88912		211
		3	84273	92937	90939	90134	88167	88900	1.0926	89025		125
$5s^2 5p^5 6d$	$^2[5/2]^o$	2	84610	93238	91272	90449	88514	89232	0.9548	89243		11
		3	84900	93476	91533	90700	88790	89496	1.2085	89535		39

use shorter basis for the ions because we calculate only lowest states. To go up in the spectrum we would need to extend the basis similar to what is done for Xe I. The analysis of the data in Tables IV, V, VI, VII, VIII and IX. show that the accuracy is generally very good in spite of very short basis.

For the Xe III ion we also included calculations which use the basis states of the Xe IV ion (column $E(N - 1)$ of Table VIII). The purpose of these calculations will be explained in the *negative ions* section below.

VII. SOME SPECIAL CASES

A. Highly excited states

One of the additional advantages of the use of V^N basis for valence states is the possibility to study highly excited states with a very short basis. To get to a highly excited state with an universal basis like B-splines one has to calculate all states of the same parity and total momentum J which are below of the state of interest. Also, the completeness of the basis deteriorates rapidly while going higher in the spectrum. V^N basis is free from these problems. To calculate highly excited states of a particular configuration it is sufficient to include into single-electron basis for valence states only states which correspond to this configuration. For example, the states

TABLE IV: Ground state removal energy (a.u.), excitation energies (cm^{-1}) and g -factors of lowest states of Xe VII ; comparison with experiment

State	J	Expt [26]		Calculations		
		E	E	g	Δ	
$5s^2$	1S	0	-7.26		-7.27	
$5s5p$	$^3P^o$	0	96141	94889	0	1252
		1	100451	99394	1.4846	1057
		2	113676	112598	1.5000	1078
$5s5p$	$^1P^o$	1	143259	146337	1.0153	-3078
	$5p^2$	0	223673	224343	0	-670
		1	234685	235008	1.5000	-323
		2	251853	252607	1.3027	-754
$5p^2$	1D	2	236100	237129	1.1962	-1029
$5p^2$	1S	0	273208	281328	0	-8120
$5s5d$	3D	1	287772	291855	0.5000	-4083
		2	288712	292896	1.1663	-4184
		3	290340	294591	1.3333	-4251
		4	307542	317647	1.0015	-10105
$5s5d$	3S	1	354833	358686	2.0000	-3853
$5s6s$	1S	0	361671	364853	0	-3182
$5p5d$	$^3F^o$	2	393792	398186	0.7405	-4394
		3	401413	406187	1.0990	-4774
		4	412567	417863	1.2500	-5296

TABLE VI: Ground state removal energy (a.u.), excitation energies (cm^{-1}) and g -factors of lowest states of Xe V; comparison with experiment

State	J	Expt [26]		Calculations		
		E	E	g	Δ	
$5s^25p^2$	3P	0	-11.7	-11.72		
$5s5p^2$		1	9292	8969	1.5000	323
		2	14127	14643	1.3744	-516
		2	28412	30169	1.1256	-1757
$5s^25p^2$	1D	2	44470	47061	0	-2591
$5s^25p^2$	1S	0	92183	88033	1.9744	4150
$5s5p^3$	$^5S^o$	2	115286	115554	0.6192	-268
	$^3D^o$	1	116097	116202	1.2256	-105
		2	119919	120152	1.3329	-233
$5s5p^3$	$^3P^o$	0	133408	134320	0	-912
		1	134575	135493	1.4078	-918
		2	134703	135579	1.3152	-876
$5s5p^3$	$^1D^o$	2	145807	147030	1.1261	-1223
$5s5p^3$	$^3S^o$	1	155518	160672	1.7362	-5154
$5s^25p5d$	$^3F^o$	2	156507	159419	0.7036	-2912
		3	160630	163534	1.0901	-2904
		4	169799	172418	1.2500	-2619
	$^1P^o$	1	169673	175704	1.1706	-6031

TABLE V: Ground state removal energy (a.u.), excitation energies (cm^{-1}) and g -factors of lowest states of Xe VI ; comparison with experiment

State	J	Expt [26]		Calculations		
		E	E	g	Δ	
$5s^25p$	$^2P^o$	1/2	-9.71	-9.72	0.6667	
$5s5p^2$		3/2	15599	15590	1.3333	9
	4P	1/2	92586	90191	2.6301	2395
		3/2	100378	97787	1.7247	2591
$5s5p^2$	2D	5/2	107205	105036	1.5629	2169
		3/2	124870	125900	0.8243	-1030
		5/2	129230	129897	1.2366	-667
$5s5p^2$	2P	1/2	141837	145429	1.1878	-3592
		3/2	159112	162903	1.3119	-3791
$5s5p^2$	2S	1/2	157996	161647	1.5155	-3651
$5s^25d$	2D	3/2	180250	186188	0.8058	-5938
		5/2	182308	188093	1.2004	-5785
	2S	1/2	223478	224641	1.9998	-1163
$5s^26s$	2S	3/2	232586	232997	1.3377	-411

of the $5s^25p^58s$ of Xe I can be calculated with good accuracy with only four states in the basis: $5s$, $5p_{1/2}$, $5p_{3/2}$ and $8s$ (see Table X). There are many lower states of same parity and total momentum J but we can easily get rid of them by not including corresponding single-electron states into the basis.

B. Negative ions

An interesting question is whether method presented in this paper can be used to calculate states of a negative

TABLE VII: Ground state removal energy (a.u.), excitation energies (cm^{-1}) and g -factors of lowest states of Xe IV

State	J	Expt [26]		Calculations		
		E	E	g	Δ	
$5s^25p^3$	$^4S^o$	3/2	-13.2	-13.27	1.8987	
$5s^25p^3$	$^2D^o$	3/2	13267	14619	0.9778	-1352
		5/2	17511	18938	1.2000	-1427
	$^2P^o$	1/2	28036	30149	0.6667	-2113
$5s5p^4$	4P	5/2	99664	99466	1.5814	198
		3/2	106923	106710	1.7055	213
		1/2	109254	109169	2.6286	85
$5s5p^4$	2D	3/2	121929	124529	0.8925	-2600
		5/2	125475	128117	1.2153	-2642
	2P	3/2	133027	135880	0.8912	-2853
$5s^25p^25d$		1/2	136796	139997	0.7788	-3201
	4F	3/2	134981	137617	0.8501	-2636
		5/2	136496	139103	1.1064	-2607
$5s^25p^25d$		7/2	141625	144013	1.2649	-2388
		9/2	145991	148958	1.3088	-2967
	2F	5/2	141824	145598	0.9889	-3774
$5s^25p^25d$		7/2	145011	148526	1.2658	-3515
	4D	1/2	145106	147933	0.4037	-2827
		3/2	146207	148762	1.1487	-2555
$5s5p^4$		5/2	148685	151840	1.1799	-3155
		7/2	155864	159785	1.2361	-3921
	2S	1/2	150737	154437	1.5219	-3700
$5s^25p^26s$	4P	1/2	157205	161777	2.3294	-4572
		3/2	165280	167775	1.6017	-2495
		5/2	170490	174875	1.4873	-4385
$5s^25p^25d$	4P	5/2	159643	165187	1.5539	-5544
		3/2	161435	169550	1.6737	-8115
		1/2	162867	169085	2.4382	-6218

TABLE VIII: Ground state removal energy (a.u.), excitation energies (cm^{-1}) and g -factors of lowest states of Xe III

State	J	Expt [26]		Calculations		
		E	g	E	g	Δ
$5s^25p^4$	3P	2	-14.38	-14.36	1.4523	-14.38
		0	8130	8313	0	-183
		1	9794	9638	1.5000	156
$5s^25p^4$	1D	2	17099	19086	1.0477	-1987
$5s^25p^4$	1S	0	36103	37280	0	-1177
$5s5p^5$	${}^3P^o$	2	98262	98847	1.4986	-585
		1	103568	104334	1.4553	-766
$5s^25p^35d$	${}^5D^o$	3	111605	110836	1.4702	769
		2	111856	111066	1.4623	790
		4	112272	111366	1.4813	906
		1	112450	111506	1.4882	944
		0	112694	112142	0	552
$5s^25p^35d$	${}^3D^o$	2	117240	118575	1.8400	-1335
		3	121230	122482	1.3114	-1252
		1	121923	123251	0.6428	-1328
$5s^25p^35d$	${}^1P^o$	1	119026	120856	1.0670	-1830
$5s^25p^36s$	${}^5S^o$	2	121476	1.95	119002	1.1889
$5s^25p^35d$	${}^3F^o$	2	124691	127328	0.8030	-2637
		3	126120	129045	1.0994	-2925
		4	130174	133970	1.1386	-3796
		1	125617	1.77	124152	1.7102
$5s^25p^36s$	${}^3S^o$	1	125617	1.77	1465	132504
	${}^3G^o$	4	127782	131307	1.1977	-3525
		3	128349	132922	0.8245	-4573
$5s^25p^35d$	${}^3G^o$	5	132160	136422	1.2000	-4262
						140435

TABLE IX: Ground state removal energy (a.u.), excitation energies (cm^{-1}) and g -factors of lowest states of Xe II

State	J	Expt [26]		Calculations		
		E	g	E	g	Δ
$5s^25p^5$	${}^2P^o$	3/2	-15.16	-15.09	1.3333	
		1/2	10537	10763	0.6667	-226
$5s5p^6$	2S	1/2	90874	2.02	91700	2.0423
$5s^25p^46s$	[2]	5/2	93068	1.56	91729	1.5639
		3/2	95064	1.38	94188	1.4084
$5s^25p^45d$	[2]	5/2	95397	1.36	95802	1.3473
		3/2	96033	1.18	96534	1.1847
$5s^25p^45d$	[3]	7/2	95438	1.42	95783	1.3940
		5/2	106475		108559	1.0537
$5s^25p^45d$	[1]	1/2	96858	0.50	97388	0.5457
		3/2	105313	1.15	107286	1.0869
$5s^25p^45d$	[4]	9/2	99405	1.31	100848	1.3093
		7/2	101536	1.11	103581	1.1524
$5s^25p^46s$	[0]	1/2	101157	2.43	100700	2.3677
$5s^25p^46s$	[1]	3/2	102799	1.59	101988	1.5811
		1/2	106906	1.79	108148	1.9490
$5s^25p^45d$	[1]	1/2	104250	0.56	104264	0.6408
		3/2	107904	1.20	109217	1.3762
$5s^25p^45d$	[0]	1/2	105948	1.36	107566	1.1311
$5s^25p^46p$	[2] ^o	3/2	111792	1.61	112248	1.6084
		5/2	111959	1.47	112286	1.4934
$5s^25p^46p$	[3] ^o	5/2	113512	1.28	114041	1.2350
		7/2	113705	1.40	114266	1.3984
$5s^25p^46p$	[1] ^o	1/2	113673	1.50	114350	1.5358
		3/2	116783	1.37	117621	1.3609

TABLE X: Energies (cm^{-1}) and g -factors of the $5s^25p^58s$ configuration of Xe I

State	J	Expt. [26]		Calculations	
		E	g	E	g
$8s [3/2]^o$	2	90805	1.465	92288	1.5000
	1	90933	1.182	92414	1.1700
$8s' [1/2]^o$	0			104063	0
	1	101426		104118	1.3300

ion. At first glance the answer is *no* because we use V^N states for the basis and negative ions are not bound in the V^N approximation. However, we may consider the following question: what is going to happen if we add one more electron to the CI calculations for a neutral atom, when basis corresponds to the neutral atom?

For atoms like xenon, which don't form negative ions, it makes more sense to consider more general question: can a basis calculated for a system of $N - 1$ valence electrons be used to calculate many electron states of a system of N electrons? This can be easily checked. Take, for example, the Xe IV ion and add one more electron in the CI calculations to get the states of Xe III. We've done this without adding any new states into the basis. Results are presented in the last column of Table VIII. We can see that the results for the ion with the basis of the other ion are almost as good as with its own basis. Accuracy is a bit lower which is a natural consequence of the worsening of the basis. Adding more states to the basis would most certainly improve the results.

This findings are not very surprising since we know that any basis set can be used in the CI calculations. For example, in Ref. [23] calculations for neutral Kr were performed with the basis corresponding to Kr IX! The only question is how many states we need to include to get reasonable results. It turns out that at least in the case of just one more electron there is no need to greatly increase the basis. This means that we can also calculate states of negative ions by using basis states of a neutral atom.

VIII. CONCLUSION

In this paper we present a method of calculation for many-electron atoms with open shells which is both accurate and very efficient. The method is based on the so called V^{N-M} approximation in which calculations start from the highly charged ion with all valence electrons removed. High accuracy is achieved by inclusion of core-valence correlations by means of MBPT. Dominating chains of higher order diagrams are included in all orders. High efficiency of the method is mostly due to the compact V^N basis set for the states of valence electrons. The method is expected to work well for atoms in which valence electrons form a separate shell (defined by the principal quantum number). This is usually the case

if valence electrons in the atomic ground state occupy s and/or p states. This covers roughly half of the periodic table of elements. Calculations for xenon and its ions illustrate the use of the method.

Acknowledgments

The work was funded in part by the Australian Research Council.

APPENDIX A: EFFICIENT WAY OF CALCULATING $\hat{\Sigma}$

The correlation correction operator $\hat{\Sigma}_1$ is defined in such a way that its average value over a wave function of a valence electron is the correlation correction to the energy of this electron:

$$\delta\epsilon_v = \langle v | \hat{\Sigma}_1 | v \rangle. \quad (\text{A1})$$

We use the following form of the single-electron wave function

$$\psi(r)_{njl} = \frac{1}{r} \begin{pmatrix} f_n(r)\Omega(\mathbf{n})_{jlm} \\ i\alpha g_n(r)\tilde{\Omega}(\mathbf{n})_{jlm} \end{pmatrix}. \quad (\text{A2})$$

Then the expression (A1) becomes

$$\begin{aligned} \delta\epsilon_v &= \int \int f_v(r) \Sigma_{ff}(r, r') f_v(r') dr dr' \\ &+ \alpha^2 \int \int f_v(r) \Sigma_{fg}(r, r') g_v(r') dr dr' \\ &+ \alpha^2 \int \int g_v(r) \Sigma_{gf}(r, r') f_v(r') dr dr' \\ &+ \alpha^4 \int \int g_v(r) \Sigma_{gg}(r, r') g_v(r') dr dr'. \end{aligned} \quad (\text{A3})$$

Note factors α^2 and α^4 in all terms except the first one. These factors make corresponding contributions to be very small. Therefore we don't usually include them. Only Σ_{ff} will be considered in this appendix and we will omit the indexes.

1. Second-order $\hat{\Sigma}$

Good efficiency in calculating of $\hat{\Sigma}$ is achieved by dividing the calculations into two steps:

1. First, all relevant Coulomb Y functions are calculated and stored on disk.
2. Then, Σ is calculated using stored Y -functions.

The Coulomb Y -function is defined as

$$Y_{knm}(r) = \int_{r_>}^{r_<} (f_n(r') f_m(r') + \alpha^2 g_n(r') g_m(r')) dr', \quad (\text{A4})$$

where $r_< = \min(r, r')$ and $r_> = \max(r, r')$. We will also need a ρ function:

$$\rho_{jl}(r) = f_j(r) f_l(r) + \alpha^2 g_j(r) g_l(r)). \quad (\text{A5})$$

Our typical coordinate grid consists of about 1000 points. Usually all of them are used to calculate Y -functions (A4). However, there is no need to keep all points for the Y and ρ -functions for consequent calculations. It turns out that very little loss of accuracy is caused by the use of a subset of points defined as every 4th point in the interval

$$1/Z \leq r \leq R_{core}.$$

By cutting off the point on short and large distances and using only every 4th point in between we reduce the number of points by an order of magnitude. Then, Coulomb integrals are calculated in an extremely efficient way

$$q_k(jlmn) = \sum_{i=1}^{\mu} \rho_{jl}(r_i) Y_{kmn}(r_i) w_i. \quad (\text{A6})$$

Here $\mu \approx 100$ is number of points on the sub-grid and w_i are weight coefficients corresponding to a particular method of numerical integration. Note that only one of two integrations for Coulomb integrals is done on a reduced sub-grid. First integration (A4) is done with the use of all points.

An expressions for $\hat{\Sigma}_1^{(2)}$ via Y -functions is

$$\Sigma_1(r, r') = \sum_{amnk} c_1(kvamn) \times \frac{f_n(r) Y_{kam}(r) Y_{kam}(r') f_n(r')}{\epsilon_v + \epsilon_a - \epsilon_m - \epsilon_n} \quad (\text{A7})$$

$$- \sum_{amnk_1 k_2} c_2(k_1 k_2 vamn) \times \frac{f_n(r) Y_{k_1 am}(r) Y_{k_2 an}(r') f_m(r')}{\epsilon_v + \epsilon_a - \epsilon_m - \epsilon_n} \quad (\text{A8})$$

$$- \sum_{amnk} c_3(kvabm) \times \frac{f_b(r) Y_{kam}(r) Y_{kam}(r') f_b(r')}{\epsilon_a + \epsilon_b - \epsilon_v - \epsilon_m} \quad (\text{A9})$$

$$+ \sum_{amnk_1 k_2} c_4(k_1 k_2 vabm) \times \frac{f_a(r) Y_{k_1 bm}(r) Y_{k_2 am}(r') f_b(r')}{\epsilon_a + \epsilon_b - \epsilon_v - \epsilon_m} \quad (\text{A10})$$

Here c_1 , c_2 , c_3 , c_4 are angular coefficients. Expressions for them can be found elsewhere [16]. Formulas (A7),(A8),(A9),(A10), correspond to diagrams 1,2,3,4 on Fig. 2. $\hat{\Sigma}_1$ is a matrix of size $\mu \approx 100$ in coordinate space. Matrix elements of $\hat{\Sigma}_1$ are calculated by

$$\begin{aligned} \langle v | \hat{\Sigma}_1 | w \rangle &= \\ \sum_{i=1, j=1}^{\mu} f_v(r_i) \Sigma_1(r_i, r_j) f_w(r_j) w_i w_j. \end{aligned} \quad (\text{A11})$$

Note that we use a two-step procedure to calculate matrix elements of $\hat{\Sigma}_1$. First, $\hat{\Sigma}_1$ matrix which is independent on valence functions is calculated, then matrix elements of $\hat{\Sigma}_1$ are calculated. To use the same approach for $\hat{\Sigma}_2$ is

impractical. As can be seen from Fig. 4 to make $\hat{\Sigma}_2$ independent on valence states one would have to make matrices of dimensions 2, 3 and 4. Therefore we just calculate matrix elements of $\hat{\Sigma}_2$ via Coulomb integrals. Corresponding expressions can be found in Ref. [16]. Coulomb integrals are calculated as in (A6).

2. All-order Σ

We use Feynman diagram technique to include higher-order correlations into direct part of $\hat{\Sigma}_1$ (diagrams 1 and 3 on Fig. 2). Corresponding expression is [9]

$$\Sigma(\epsilon, r_i, r_j) = \sum_{nm} \int \frac{d\omega}{2\pi} G_{ij}(\epsilon + \omega) Q_{im} \tilde{\Pi}_{mn}(\omega) Q_{nj}. \quad (\text{A12})$$

Here $\tilde{\Pi}$ is “screened polarization operator”

$$\tilde{\Pi} = \Pi[1 - Q\Pi]^{-1},$$

Π is polarization operator

$$\Pi(\omega) = \sum_a \psi_a [G(\epsilon_a + \omega) + G(\epsilon_a - \omega)] \psi_a,$$

G is Green function

$$(\hat{h}_1 - \epsilon)G(r, r') = -\delta(r - r'),$$

and Q is Coulomb interaction

$$Q_{ij} = e^2 / (r_i - r_j).$$

The details of calculation of $\hat{\Sigma}_1^{(\infty)}$ can be found elsewhere [7, 9]. Here we only want to mention that operators $\tilde{\Pi}$, Π , G and Q are matrices of size $\mu \approx 100$ in coordinate space. Therefore calculation of $\hat{\Sigma}_1^{(\infty)}$ involves manipulation of matrices of relatively small size. If we also recall that $\hat{\Sigma}_1$ does not depend on valence states and needs to be calculated only once then the efficiency of its calculation is quiet satisfactory.

Higher-order correlations in exchange diagrams for $\hat{\Sigma}_1$ (diagrams 2 and 4 on Fig. 2) and for all diagrams for $\hat{\Sigma}_2$ are included via screening factors as explained in the text.

- [1] J. S. M. Ginges and V. V. Flambaum, Physics Reports, **397** 63 (2004).
- [2] J. K. Webb, V. V. Flambaum, C. W. Churchill, M. J. Drinkwater, and J. D. Barrow, Phys. Rev. Lett. **82**, 884 (1999); J. K. Webb, M. T. Murphy, V. V. Flambaum, V. A. Dzuba, J. D. Barrow, C. W. Churchill, J. X. Prochaska, and A. M. Wolfe, Phys. Rev. Lett. **87**, 091301 (2001); M. T. Murphy, J. K. Webb, V. V. Flambaum, V. A. Dzuba, C. W. Churchill, J. X. Prochaska, J. D. Barrow, and A. M. Wolfe, Mon. Not. R. Astron. Soc. **327**, 1208 (2001);
- [3] E. J. Angstmann, V. A. Dzuba, V. V. Flambaum, Phys. Rev. A, **70**, 014102 (2004); J. Angstmann, V. A. Dzuba, V. V. Flambaum, A. Yu. Nevsky, and S. G. Karshenboim, J. Phys. B: At. Mol. Phys. **39** 1937 (2006).
- [4] K. Beloy, U. I. Safranova, and A. Derevianko, Phys. Rev. Lett. **97**, 040801 (2006); E. J. Angstmann, V. A. Dzuba, V. V. Flambaum, Phys. Rev. Lett. **97** 040802 (2006); Phys. Rev. A, **74** 023405 (2006).
- [5] A. Landau, E. Eliav, Y. Ishikawa, U. Kaldor, J. Chem. Phys. **114** 2977 (2001); E. Eliav, A. Landau, Y. Ishikawa, U. Kaldor, J. Phys. B: At. Mol. Phys. **35**, 1693 (2002).
- [6] V. A. Dzuba, V. V. Flambaum, P. G. Silvestrov, O. P. Sushkov, J. Phys. B: At. Mol. Phys. **20**, 1399 (1987).
- [7] V. A. Dzuba, V. V. Flambaum, O. P. Sushkov, Phys. Lett. A., **140**, 493-497 (1989); Phys. Lett. A, **141**, 147-153 (1989); V. A. Dzuba, V. V. Flambaum, A. Ya. Kraftmakher, O. P. Sushkov, Phys. Lett. A, **142**, 373-377 (1989).
- [8] S. A. Blundell, W. R. Johnson, and J. Sapirstein, Phys. Rev. Lett. **65**, 1411 (1990); S. A. Blundell, J. Sapirstein, and W. R. Johnson, Phys. Rev. D **45**, 1602 (1992).
- [9] V. A. Dzuba, V. V. Flambaum, J. S. M. Ginges, Phys. Rev. D, **66**, 076013 (2002).
- [10] V. A. Dzuba, V. V. Flambaum, P. G. Silvestrov, O. P. Sushkov, J. Phys. B: At. Mol. Phys. **20**, 3297-3311 (1987).
- [11] M. G. Kozlov, S. G. Porsev, and W. R. Johnson, Phys. Rev. A 64, 052107 (2001).
- [12] Hsiang-Shun Chou and W.R. Johnson, Phys. Rev. A **56**, 2424 (1997); S.A. Blundell, W.R. Johnson, and J. Sapirstein, Phys. Rev. A **42**, 3751 (1990).
- [13] S.A. Blundell, W.R. Johnson and J. Sapirstein, Phys. Rev. A **43**, 3407 (1991); A. Landau, E. Eliav, Y. Ishikawa, U. Kaldor, J. Chem. Phys. **121**, 6634 (2004).
- [14] K.T. Cheng, M.H. Chen, W.R. Johnson and J. Sapirstein, Phys. Rev. A **50**, 247 (1994); K. T. Cheng, M. H. Chen, Rad. Phys. Chem. **75**, 1753 (2006); P. Bogdanovich, D. Majus, T. Pakhomova, Phys. Scr. **74** 558 (2006).
- [15] I. P. Grant, Comput. Phys. Commun. **84**, 59 (1994).
- [16] V. A. Dzuba, V. V. Flambaum, and M. G. Kozlov, Phys. Rev. A, **54**, 3948 (1996).
- [17] V. A. Dzuba and W. R. Johnson, Phys. Rev. A, **57**, 2459 (1998).
- [18] V. A. Dzuba, V. V. Flambaum, M. G. Kozlov, and S. G. Porsev, J. Exp. Theor. Phys., **87**, 885 (1998).
- [19] I. M. Savukov, W. R. Johnson, Phys. Rev. A **65**, 042503 (2002).
- [20] I. M. Savukov, W. R. Johnson, H. G. Berry, Phys. Rev. A **66**, 052501 (2002).
- [21] I. M. Savukov, J. Phys. B: At. Mol. Phys. **36**, 2001 (2003).
- [22] V. A. Dzuba, J. S. M. Ginges, Phys. Rev. A, **73** 032503 (2006); V. A. Dzuba and V. V. Flambaum, J. Phys. B: At. Mol. Opt. Phys. **40** 227 (2007).
- [23] V. A. Dzuba, Phys. Rev. A, **71**, 032512 (2005).
- [24] V. A. Dzuba and V. V. Flambaum, Phys. Rev. A, **71**,

- 052509 (2005).
- [25] V. A. Dzuba, Phys. Rev. A, **71**, 062501 (2005).
- [26] NIST Atomic Spectra Database on Internet,
http://physics.nist.gov/cgi-bin/AtData/main_asd.